Polymer 54 (2013) 4446–4454

Contents lists available at SciVerse ScienceDirect

Polymer

journal homepage: www.elsevier.com/locate/polymer

The behaviour of honeycomb film formation from star polymers with various fluorine content

Zhou Zhang [a,b], Timothy C. Hughes [b], Paul A. Gurr [a], Anton Blencowe [a], Hemayet Uddin [a], Xiaojuan Hao [b,*], Greg G. Qiao [a,*]

[a] Department of Chemical and Biomolecular Engineering, University of Melbourne, Parkville, VIC 3010, Australia
[b] Materials Science and Engineering, Commonwealth Scientific and Industrial Research Organization (CSIRO), Clayton, VIC 3168, Australia

ARTICLE INFO

Article history:
Received 23 April 2013
Received in revised form
12 June 2013
Accepted 13 June 2013
Available online 25 June 2013

Keywords:
Fluorinated star polymers
Honeycomb films
Physical properties

ABSTRACT

A series of poly((*1H,1H*-pentafluoropropyl acrylate)-*ran*-(methyl methacrylate)) (poly(PFPA-*ran*-MMA)) star polymers with varying fluorine content were prepared *via* the core-first approach using atom-transfer radical polymerisation (ATRP). Subsequently, the star polymers were used to prepare honeycomb films on both planar and non-planar surfaces *via* the 'Breath Figures' technique using a static casting method. The fluorine content of the star polymers was observed to influence the morphology of the honeycomb structures and the formation of non-cracking honeycomb films on non-planar surfaces. Moreover, the average pore diameter of the honeycomb films was found to decrease with increasing fluorine content, as well as increasing polymer concentration in the casting solution or decreasing humidity during casting. The increasing fluorine content of the star polymers was also found to result in a decrease in their glass transition temperatures and Young's modulus values.

© 2013 Elsevier Ltd. All rights reserved.

1. Introduction

Highly ordered honeycomb (HC) patterned films formed *via* the 'Breath Figures' (BF) technique [1,2] are of great interest as a result of their wide range of specialised technological applications, including biosensors [3–5], membranes for purification and separation [6,7], tissue engineering [8], photonic band gap [9] and electronics [10]. The BF technique was first introduced by Rayleigh and co-workers [11], whereby water droplets were utilised as templates for polymers to form self-assembled, highly ordered HC films. Numerous (macro)molecular architectures have been used with the BF technique to obtain ordered macroporous and microporous structures, including rod-coil block copolymers [12–15], conjugated polymers [16], amphiphiles [17,18], dendronized polymers [19], star polymers [15,20,21], polyoxometalates [22], and small molecules [23]. In addition, various approaches have been established to cast HC films, including, but not limited to, computer-driven [24], dynamic [15,25–31] and static casting methods [20,21,32–34]. The advantage of the computer-driven casting system is that temperature, air velocity, relative humidity, and film thickness can be precisely and independently controlled while the formation of HC films can be monitored using an in-line optical microscope and video recording system. In comparison, the most commonly adopted approach, known as the dynamic casting method, is a simple approach for the fabrication of HC films. However, its main drawback is the unpredictable turbulence of moist air flow, which may induce deformation of the resulting structures. This issue can be eliminated by using the static casting method, which operates without the flow of moist air, although relatively high humidities are required to form HC films.

Although HC structured films formed from numerous polymers have been reported, to date, limited studies have investigated the formation of fluorinated HC films. Fluorinated polymers have attracted significant attention as a result of their unique properties, including extremely low surface energy and high hydrophobicity, which imparts excellent water and oil repellence, and chemical and thermal stability [35–38]. Fluorinated materials have thus found applications in high performance coatings on various substrates, displaying excellent protection against corrosion, weathering, and environmental pollutants [39–42]. As a result of their biological inertness, fluorinated polymers have also been used as ophthalmic biomaterials [43,44].

Our earlier work showed that when highly dendronised star polymers with peripheral fluorinated groups were used for honeycomb structure formation, 'cylinder-like' pore structures were formed [26]. Yabu et al. [24,45] demonstrated that fluorinated HC

* Corresponding authors.
E-mail addresses: Xiaojuan.Hao@csiro.au (X. Hao), gregghq@unimelb.edu.au (G.G. Qiao).

0032-3861/$ – see front matter © 2013 Elsevier Ltd. All rights reserved.
http://dx.doi.org/10.1016/j.polymer.2013.06.033

films and their 'skin-off' pincushion structures displayed different hydrophobicities. Furthermore, they also prepared HC patterned films with submicron pore diameters *via* a computer-driven casting system [24]. These nanometre pore-sized HC patterned films were optically transparent and exhibited superhydrophobicity. Recently, we reported the formation of HC films from perfluoropolyether-based star polymers and micelles on both planar and non-planar surfaces [21]. Although these studies have highlighted the unique abilities of fluorinated polymers and their resulting HC structures, investigation of the effect of the extent of fluorination of the polymers on the formation of HC films and their physical properties have so far been limited. Our recent studies have discovered that increasing the PFPA content of a star polymer decreases its Young's modulus (E), effectively improving its ability to form non-cracking HC films on non-planar surfaces. In addition, these results indicated that E serves as a better indicator than a polymer's glass transition temperature (T_g), in terms of predicting the polymer's ability to form non-cracking HC films on non-planar surfaces [20]. Therefore, there is a need to study the influence of fluorine content in the polymer precursors on their formation of HC films in general.

In this paper, we introduce a library of T_g tuneable fluorinated star polymers with various arm numbers (4, 6 and 21) prepared by the core-first approach and atom-transfer radical polymerisation (ATRP) of a fluorinated acrylate, pentafluoropropyl acrylate, and methyl methacrylate. The effect of star polymer composition (i.e., fluorine content) and architecture (number of arms) on the formation of HC films on both planar and non-planar surfaces, and the physical properties of the resulting films were studied. This study also provides further experimental evidence to validate the hypothesis of the role of E in the formation of non-cracking HC films on non-planar surfaces [20].

2. Experimental

2.1. Materials

1H,1H-Pentafluoropropyl acrylate (PFPA) (Fluorochem, >97%) and activated neutral aluminium oxide (Al_2O_3) (Merck) were used as received. Methyl methacrylate (MMA) (99%) was purchased from Sigma–Aldrich, stirred with inhibitor remover (Sigma–Aldrich) for 18 h and then filtered before use. β-Cyclodextrin (β-CD) (98%), pentaerythritol (≥99.9%), dipentaerythritol (technical grade), 2-bromo-2-methyl-propanoyl bromide (98%), copper(I) bromide (CuBr) (98%), lithium bromide (LiBr) (≥99%), anhydrous dioxane (≥99.8%), sodium bicarbonate ($NaHCO_3$), magnesium sulphate ($MgSO_4$) (anhydrous, ≥ 99.5%), *N,N,N′,N′N″*-pentamethyldiethylenetriamine (PMDETA) (99%), and *N*-methyl-2-pyrrolidinone (NMP) (99.5%) were purchased from Sigma–Aldrich and used as received. Toluene (HPLC grade), *N,N*-dimethylformamide (DMF), dichloromethane (CH_2Cl_2) (AR grade), chloroform ($CHCl_3$) (AR grade), ethanol (EtOH), and methanol (MeOH) (AR grade) were purchased from Chem-Supply and used as received. Tetrahydrofuran (THF) (HPLC grade) was purchased from Burdick and Jackson. Anhydrous THF was obtained by distillation under argon from sodium benzophenone ketyl. Triethylamine (TEA)

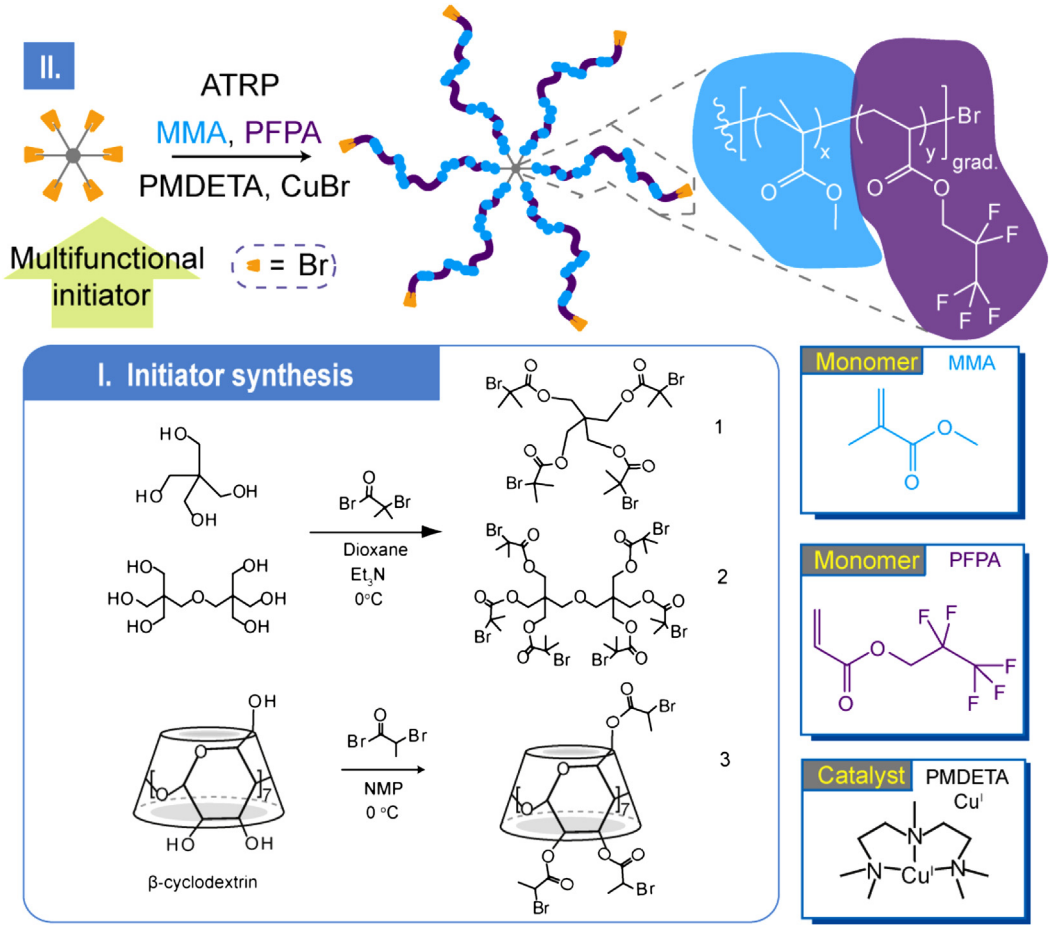

Scheme 1. Synthesis of (i) multifunctional initiators **1**, **2**, and **3**, and (ii) fluorinated star polymers with varying PFPA monomer content using the multifunctional initiators *via* the core-first approach and ATRP. The PFPA monomer content was controlled by varying the ratio of methyl methacrylate (MMA) to pentafluoropropyl acrylate (PFPA).

(Chem-Supply, LR grade) was distilled from CaH_2 prior to use. Deuterated chloroform ($CDCl_3$) + 1% v/v tetramethylsilane (TMS) (D, 99.8%) was purchased from Cambridge Isotope Laboratories. Argon (UHP) was purchased from BOC, Australia. Copper TEM grids (300 mesh) were purchased from ProSciTech Pty Ltd.

2.2. Measurements

Gel permeation chromatography (GPC) was performed on a Shimadzu liquid chromatography system fitted with a Wyatt DAWN HELEOS LS detector ($\lambda = 658$ nm), Shimadzu RID-10 refractometer ($\lambda = 633$ nm) and Shimadzu SPD-20A UV–Vis detector, using three identical Polymer Laboratories PLgel columns (5 μm, MIXED-C) and DMF with 0.05 M LiBr (70 °C, 1 mL/min) as the mobile phase. ASTRA software (Wyatt Technology Corp.) was used to process the data using either known *dn/dc* values or based upon 100% mass recovery of the polymer where the *dn/dc* value was unknown. ^{1}H and ^{13}C NMR spectroscopic analysis was performed on a Varian Unity Plus 400 spectrometer operating at 400 and 100 MHz, respectively. Deuterated chloroform ($CDCl_3$) with 1% TMS was used as solvent and internal reference, respectively. Differential scanning calorimetry (DSC) was performed on 2920 Modulated DSC (TA Instruments). TA Universal Analysis 2000 was used to process the data for determination of T_g. Each sample was heated and cooled at a rate of 10 °C/min and this was repeated twice. The T_g values were recorded on the second heating run. Contact angle measurements were conducted on Data Physics OCA 20 Tensiometer. Measurements were recorded by OCA software, using a sessile drop profile. Atomic force microscopy (AFM) was performed on Asylum Research MFP-3D AFM. Nonporous thin films were prepared by depositing 20 μL of a polymer solution on a clean microscope glass slide and allowing the solvent to evaporate at room temperature. The Young's modulus (E) of the thin films was measured in force mode using pyramid shaped silicon cantilevers (Model AC240Ts, 70 (50–90) kHz, 2 (0.5–4.4) N/m; AC200Ts, 115 (75–175) kHz, 9.7 (4.0–22.3) N/m; AC160TS, 300 (200–400) kHz, 42 (12–103) N/m, Asylum Research). The Hertzian contact mechanics model [46–48] was applied on approach curves to obtain *E*. HC films were imaged by scanning electron microscopy (SEM) using a FEI Quanta 200 ESEM FEG. Samples were coated with gold using a Dynavac Mini sputter coater prior to imaging. Image-Pro® software was employed to analyse SEM images of HC films and 2D Fast Fourier Transform (FFT) images.

2.3. Synthesis of tetra-functional initiator **1**

Pentaerythritol (2.00 g, 14.7 mmol, 1 equiv.), TEA (12.3 mL, 88.2 mmol, 6 equiv.) and anhydrous dioxane (100 mL) were added to a flask under argon. The mixture was cooled to −18 °C and 2-bromo-2-methylpropanoyl bromide (10.9 mL, 88.2 mmol, 6 equiv.) dissolved in anhydrous THF (20 mL) was added dropwise over a period of 1 h. The resulting mixture was stirred at room temperature for 12 h and then diluted with dichloromethane (400 mL) and stirred for another 30 min. The organic solution was washed with 2 M HCl (2 × 250 mL), saturated $NaHCO_3$ (2 × 250 mL), dried ($MgSO_4$), filtered, and concentrated *in vacuo* to afford a yellow solid. The solid was recrystallised from hot ethanol, cooled at 0 °C and filtered to afford initiator **1** as a colourless crystalline solid, 8.82 g (79%). ^{1}H NMR ($CDCl_3$, 400 MHz): δ_H 1.94 (*s*, 24H, 8C***H***$_3$), 4.33 (*s*, 8H, 4C***H***$_2$) ppm. ^{13}C NMR ($CDCl_3$, 100 MHz): δ_C 30.6 (8***C***H$_3$), 43.6 (***C***(CH$_2$)$_4$), 55.2 (4***C***Br), 62.9 (4***C***H$_2$O), 170.9 (4***C***=O) ppm.

2.4. Synthesis of hexa-functional initiator **2**

Dipentaerythritol (1.60 g, 6.28 mmol, 1 equiv.), TEA (8.00 mL, 56.6 mmol, 9 equiv.) and anhydrous dioxane (100 mL) were added to a flask under argon. The mixture was cooled to −18 °C and 2-bromo-2-methylpropanoyl bromide (7.00 mL, 56.6 mmol, 9 equiv.) dissolved in anhydrous dioxane (50 mL) was added dropwise over a period of 1 h. The resulting mixture was stirred at room temperature for 20 h and then diluted with chloroform (400 mL) and stirred for another 30 min. The organic solution was washed with 2 M HCl (2 × 200 mL), saturated $NaHCO_3$ (2 × 200 mL), aqueous 5 wt% $NaHCO_3$ (2 × 200 mL), dried ($MgSO_4$), filtered, and concentrated *in vacuo* to afford a dark orange oil. The product that crystallised upon cooling at 0 °C was recrystallised from hot ethanol, cooled at 0 °C and filtered off to afford initiator **2** as a colourless crystalline solid, 5.45 g (76%). ^{1}H NMR ($CDCl_3$, 400 MHz): δ_H 1.93 (*s*, 36H, 12C***H***$_3$), 3.60 (*s*, 4H, C***H***$_2$OC***H***$_2$), 4.29 (*s*, 12H, 6C***H***$_2$O) ppm. ^{13}C NMR ($CDCl_3$, 100 MHz): δ_C 30.7 (12***C***H$_3$), 44.3 (2***C***(CH$_2$)$_4$), 55.5 (6***C***Br), 63.2 (6***C***H$_2$O), 69.1 (2***C***H$_2$O), 170.9 (6***C***=O) ppm.

Table 1
Characterisation of 4, 6, and 21 armed fluorinated star polymers.

Star polymers[a]	M_w[b] (kDa)	PDI[c]	T_g[d] (°C)	PFPA monomer content[e] (mol%)	E[f] (GPa)
4S$_1$	76.8	1.05	69.5	25.8	4.86
4S$_2$	58.7	1.13	49.7	35.0	4.15
4S$_3$	39.6	1.08	44.5	42.0	3.88
4S$_4$	90.5	1.05	20.8	58.6	3.54
6S$_1$	60.9	1.23	57.3	30.0	4.40
6S$_2$	296.8	1.26	52.3	33.0	4.25
6S$_3$	88.6	1.08	41.0	41.0	3.90
6S$_4$	88.5	1.08	26.7	54.5	3.62
21S$_1$	66.5	1.07	94.5	4.4	5.07
21S$_2$	225.0	1.15	74.1	20.5	4.63
21S$_3$	61.6	1.20	55.4	32.5	4.34
21S$_4$	242.5	1.22	53.5	33.0	4.26
21S$_5$	196.5	1.11	21.8	57.2	3.50

[a] **4S**, **6S**, and **21S** represent 4, 6, and 21 armed star polymers, respectively.
[b] Weight-average molecular weight of star polymers determined by GPC-MALLS and based upon the assumption of 100% mass recovery.
[c] Polydispersity index determined by GPC.
[d] Glass transition temperature determined by DSC.
[e] Mol% based upon ^{1}H NMR spectroscopic analysis.
[f] Young's modulus determined by AFM on planar films.

2.5. Synthesis of β-CD-Br$_{21}$ multifunctional initiator **3**

This compound was prepared according to the procedure described by Li and Xiao [49]. ^{1}H NMR ($CDCl_3$, 400 MHz): δ_H 1.87 (*m*,

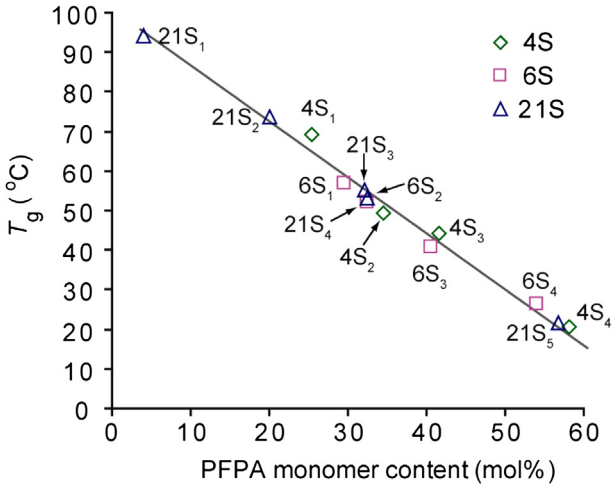

Fig. 1. The relationship between PFPA content and glass transition temperature (T_g) of the fluorinated star polymers.

63H, 21C***H***$_3$), 3.75–5.56 (*m*, 70H, 21C***H***Br & 35C***H***O & 7C***H***$_2$O) ppm; ^{13}C NMR ($CDCl_3$, 100 MHz): δ_C 21.5 (21***C***H_3), 39.5 (21***C***Br), 63.9 (7***C***-6), 70.2-74.8 (7***C***-2, 7***C***-3, 7***C***-4, 7***C***-5), 96.3 (7***C***-1), 169.1 (7***C***=O) ppm.

2.6. Synthesis of 4 armed fluorinated star polymers (*4S*)

A solution of initiator **1** (27.0 mg, 36.7 μmol, 1 equiv.), PMDETA (8.0 μL, 36.7 μmol, 1 equiv.), PFPA (1.14 mL, 7.35 mmol, 200 equiv.) and MMA (2.35 mL, 21.75 mmol, 600 equiv.) in toluene (5.4 mL) was added to a Schlenk tube (oven-dried at 110 °C for 48 h) complete with a stirrer bar. The mixture was subjected to three freeze-pump-thaw cycles and then back-filled with argon. The solution was frozen again in liquid N_2 and CuBr (5.0 mg, 36.7 μmol, 1 equiv.) was added under a flow of argon. Another three freeze-pump-thaw cycles were performed and then the Schlenk tube was back-filled with argon and left at room temperature with stirring for 10 min to ensure homogeneity. The reaction mixture was then heated at 60 °C for 10 h. An aliquot (0.2 mL) was taken *via* a gas-tight syringe at t_0 and after 10 h to determine monomer conversion. The reaction mixture was cooled to room temperature, diluted with chloroform (3 mL) and passed through a plug of basic Al_2O_3 to remove the copper catalyst. The filtrate was precipitated into methanol (50 mL) and the precipitate was collected *via* centrifugation and dried *in vacuo* (50 °C, 0.1 mbar) to afford the star polymer as a white solid, 2.74 g (73.4%) (ESI, Fig. S1). The composition of PFPA and MMA repeating units in the star polymers was varied by changing the monomer feed ratio (ESI, Table S1).

2.7. Synthesis of 6 armed fluorinated star polymers (*6S*)

These star polymers were synthesised in an identical fashion to that described for the 4 armed star polymers with the exception that initiator **2** was used in place of initiator **1**. The composition of PFPA and MMA repeating units in the star polymers was varied by changing the monomer feed ratio (ESI, Table S2).

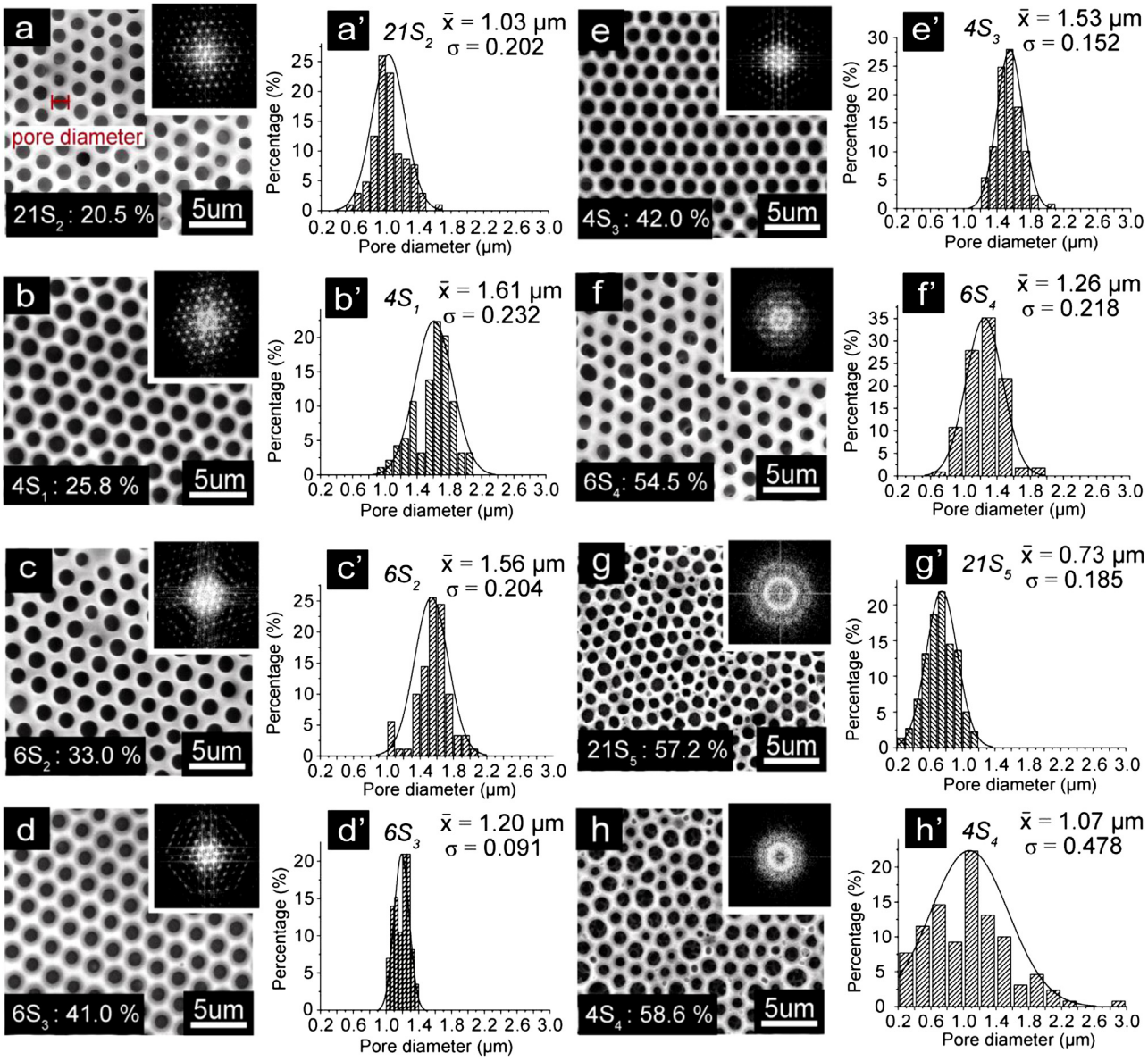

Fig. 2. (a–h) SEM images of HC films formed from star polymers. Insets: 2D FFT images of HC patterned films and corresponding star polymer and their PFPA content expressed as mol%; (a′–h′) Histograms showing pore diameter distributions of HC films shown in **a**–**h**, respectively, including average pore diameters ($\bar{x}$) and standard deviations (σ).

2.8. Synthesis of 21 armed fluorinated star polymers (**21S**)

These compounds were prepared according to the procedure described previously by Zhang et al. [20].

3. Honeycomb film preparation

3.1. Planar surface casting

HC films were prepared by first stabilising the conditions of a casting environment at *ca.* 30 °C and the desired relative humidity (R.H.) between the range of 70 ± 5–90 ± 5%. The fluorinated star polymers were dissolved in chloroform at the desired concentration (3, 5, and 10 mg/mL) and 20 μL of the solution was deposited onto a circular glass cover slip and the solvent and water were left to evaporate in the casting environment (Scheme S1).

3.2. Non-planar surface casting

The conditions of the casting environment were set to *ca.* 30 °C and a relative humidity of 70 ± 5%. A TEM grid was placed onto a glass cover slip and 20 μL of the star polymer solution in chloroform (5 mg/mL) was deposited on top of the grid and the solvent and water were left to evaporate in the casting environment (Scheme S2).

4. Results and discussion

4.1. Preparation of star polymers

Studies have shown that multifunctional ATRP initiators have high initiation efficiency and provide good control over the polymer chain growth from multiple initiation sites simultaneously [50–53]. Therefore, to synthesise star polymers with well-defined structures, the core-first approach [54] was used to synthesise a series of star polymers with tuneable T_g values *via* ATRP of vinyl monomers (i.e. PFPA and MMA) from multifunctional initiators, thus forming the arms of the star polymers (Scheme 1). Although the number of arms in star polymers can be experimentally determined through cleaving experiments, in this work it was assumed that controlled polymer growth occurred from all possible initiation sites. This approach allows for the preparation of well-defined star polymers with a precise number of arms, which can be controlled by the number of initiating moieties present on the multifunctional initiator (core). This is, of course, dependent on equal reactivity for the initiating sites, as well as a higher rate of initiation relative to propagation in the polymerisation process. The benefits of this approach include high monomer conversions and facile isolation of the pure star polymers from the polymerisation solution. In this study, 4, 6, and 21 armed fluorinated star polymers were synthesised using the multifunctional initiators **1**, **2**, and **3**, respectively, *via* random copolymerisation of PFPA and MMA (Scheme 1). Based upon the known reactivity ratios of the monomers it is likely that the arms of the star polymers adopt a gradient structure with a gradual compositional change from high MMA content to high PFPA content in the repeating units towards the periphery of the star polymers ($r_{MMA} = 2.42$ and $r_{PFPA} = 0.30$) [20].

The synthesis of the star polymers with varying PFPA content was confirmed by ^{1}H NMR spectroscopic analysis and GPC (ESI, Fig. S1). The polymerisation was well controlled over a range of molecular weights, as indicated by the narrow polydispersities (Table 1). The T_g values of the star polymers were determined by DSC, varying from 20.8 to 94.5 °C depending upon the polymer composition. The PFPA content was simultaneously varied from 4.4 to 58.6%, as determined by ^{1}H NMR spectroscopic analysis (ESI, Fig. S1). A significant increase in PFPA content resulted in a decrease in T_g, independent of the number of arms (f) of the star polymer

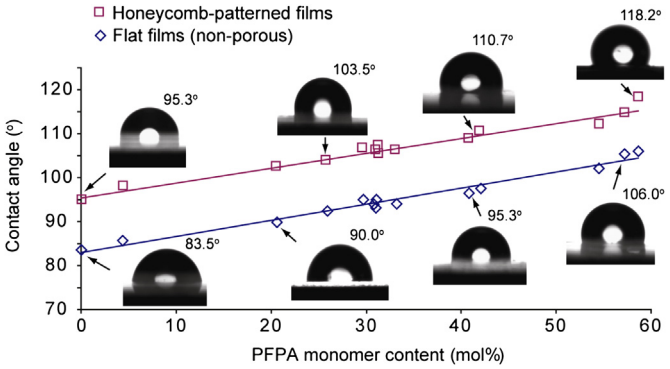

Fig. 3. Contact angle as a function of PFPA content, and selected images used to calculate the contact angles.

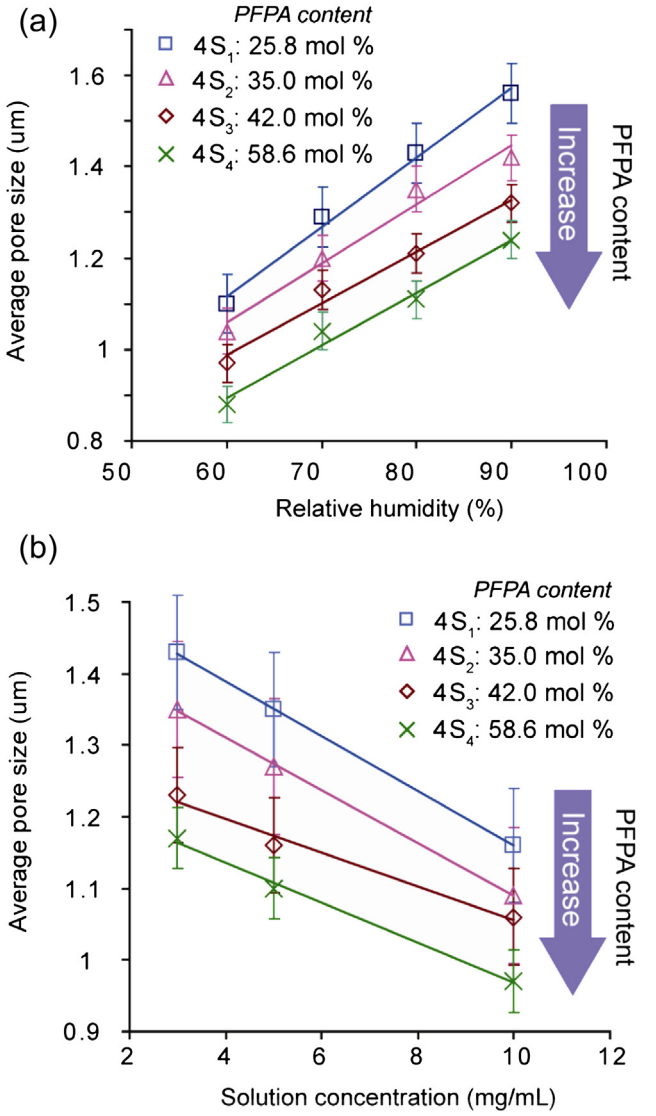

Fig. 4. Effect of (a) relative humidity: star polymer solutions were prepared in $CHCl_3$ (3 mg/mL) and cast under relative humidities ranging from 60 to 90%; and (b) concentration of polymer in casting solution: star polymer solutions were prepared in $CHCl_3$ with different concentrations (3, 5, and 10 mg/mL) and cast under 70% relative humidity.

(Fig. 1), which provides a facile approach to tune the polymer's T_g. Therefore, polymers with a range of T_g values could be easily prepared according to the PFPA content (Table 1).

5. Formation of honeycomb (HC) films from fluorinated star polymers

5.1. Planar surfaces

HC films were fabricated by casting dilute solutions of the fluorinated star polymers (Table 1) on glass cover slips using a static casting method. Representative images of HC films prepared from the star polymers (**4S$_{1,3,4}$**, **6S$_{2-4}$** and **21S$_{2,5}$**) with a broad range of PFPA content are shown in Fig. 2. Measurement of the pore diameters (as depicted in Fig. 2a) of the HC films provided average pore diameters ($\bar{x}$) of 0.7–1.6 μm (Fig. 2a′–h′). The pore diameter distribution of the HC films varied greatly depending on the polymer. For example, star polymer **6S$_3$** (Fig. 2d) had the narrowest pore diameter distribution with a standard deviation (σ) of 0.091 (Fig. 2d′), while **4S$_4$** had the broadest distribution, with an σ of 0.478 (Fig. 2h and h′). However, a narrow pore diameter distribution does not necessarily guarantee a uniform HC pattern. Whereas more uniform HC structures were observed from star polymers with PFPA contents of <50 mol%, the HC structures became less regular as the PFPA content increased. 2D Fast Fourier Transform (FFT) [55] of the images in Fig. 2 was used to illuminate the regularity of the HC patterns (inset of Fig. 2a–h and ESI, Fig. S2) [56–58]. The 2D FFT illuminates discrete order characteristics of either a well-ordered hexagonal arrangement morphology (2D FFT inset: Fig. 2a–e) or a less regular morphology shown as rings (2D FFT inset: Fig. 2f–h), confirming the pore regularity. Images that showed the most perfect hexagonal pore ordering, in terms of pore arrangement and shape, were obtained from polymers **4S$_{1,3}$**, **6S$_{2,3}$** and **21S$_2$** (Fig. 2a′–e′), while the less ordered HC films obtained from star polymers with higher PFPA content led to less detailed singularly bright images (Fig. 2f–h). Thus, the regularity of the resulting HC films is related to the PFPA content of the star polymers, with well patterned HC films more likely to be obtained from star polymers with <50 mol% PFPA content (ESI, Fig. S2).

5.2. Contact angle measurement

Contact angles were measured on both non-porous films and HC patterned films formed from the fluorinated star polymers. Firstly, flat films were prepared by casting polymer solutions onto glass cover slips and allowing the solvent to evaporate in a dry (i.e., non-humid) ambient environment. As expected, increasing the PFPA content of the star polymers led to an increase in the contact angle of the resulting planar films from 90 to 106° (Fig. 3). In general, the contact angles of the HC films were *ca.* 12° higher than non-porous films prepared from the same star polymer (Fig. 3), which demonstrates that the HC topography enhances the hydrophobicity of the films. The linear relationships imply that the contact angle of a

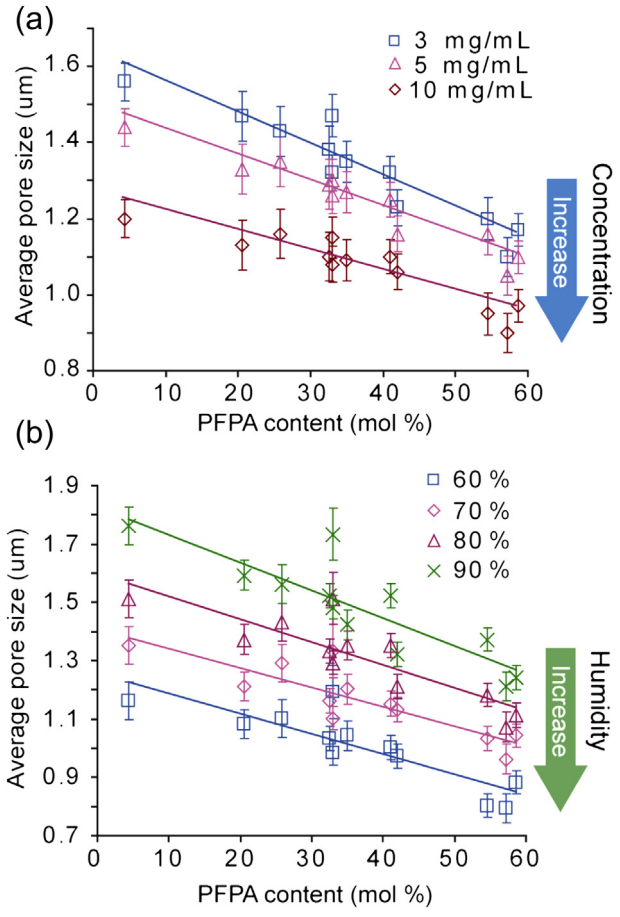

Fig. 5. Correlation between HC film pore diameter and star polymer PFPA content of all 4, 6, and 21 armed star polymers.

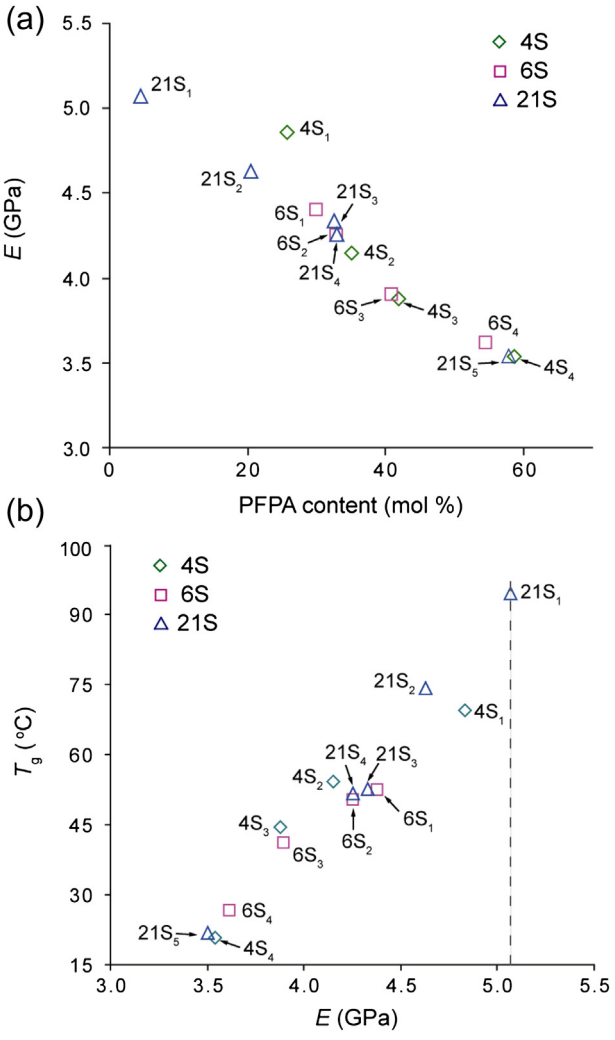

Fig. 6. (a) Correlation between Young's modulus (E) and star polymer PFPA content. (b) Glass transition temperature (T_g) versus Young's modulus (E) of the star polymers.

HC film prepared from a particular fluorinated star polymer can be predicted by measurement of the contact angle of its flat film counterpart.

5.3. Effect of humidity and casting solution concentration on pore diameter at different PFPA content

It is well known that the casting humidity and polymer solution concentration have a strong influence on pore formation for HC films [2,59,60]. To investigate if the formation of HC films from star polymers with various PFPA content follow the same principles, HC films were prepared from star polymer solutions (3 mg/mL in $CHCl_3$) at 60, 70, 80, and 90% R.H, respectively, on glass cover slips. HC structures were successfully formed over all of the R.H. employed, and as previously reported [61–63], the pore diameters were found to increase with increasing humidity (Fig. 4a). The average pore diameters of HC films cast from **$4S_{1-4}$** are shown as representative examples. Regardless of the PFPA content of the star

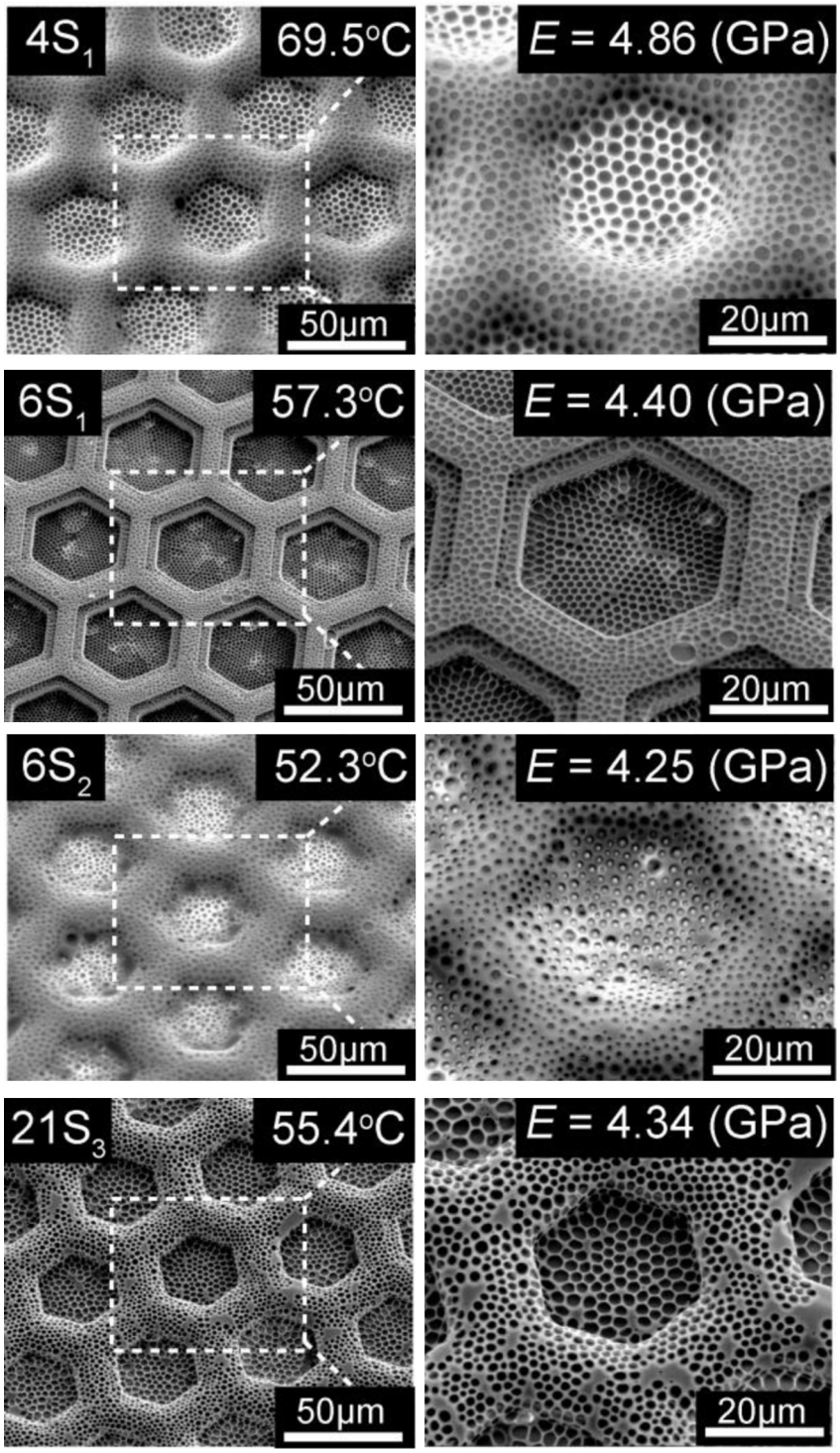

Fig. 7. SEM images of non-planar HC patterned films formed from star polymers **$4S_1$**, **$6S_1$**, **$6S_2$** and **$21S_3$** with varying PFPA content ranging from 32.5 to 25.8 mol% and T_g values ranging from 52.3 to 69.5 °C.

polymers a similar increasing rate in pore diameter was observed for the HC films with increasing humidity. Importantly, star polymers with relatively high PFPA content led to HC structures with smaller pore diameters. Subsequently, the average pore diameter formed from different solution concentrations was investigated by casting films at various polymer concentrations (3, 5, and 10 mg/mL in chloroform) under a fixed R.H. (70%). The results (Fig. 4b) indicate that with the same number of arms ($f = 4$), smaller pore diameters were obtained from star polymers with a higher PFPA content regardless of the star polymers concentration. Moreover, for star **4S$_{1-4}$** with different PFPA content, the pore diameters of the resulting HC films were found to decrease at a similar rate with increasing solution concentration. For HC films formed from other **6S** and **21S** polymers, similar humidity and solution concentration trends were observed at various PFPA content (ESI, Figs. S3 and S4).

5.4. Effect of PFPA content on pore diameter of HC films

The PFPA content of the star polymers was plotted against the average pore diameters of the resulting HC films cast at different polymer concentrations (Fig. 5a) and humidities (Fig. 5b). At different polymer concentrations (3, 5, and 10 mg/mL), the average pore diameter of the HC films prepared from the star polymers, despite different *f* values, followed a similar decreasing trend as a function of PFPA content. Similar trends were also observed for the films formed under varying relative humidities (Fig. 5b). The decrease in the average pore diameter could be attributed to the increasing hydrophobicity with greater PFPA content, which may accelerate the polymer aggregation/precipitation rate at the solution/water interface during casting. Importantly, these observations suggest that the PFPA content of the star polymers is more influential on the pore diameters of the resulting HC films than their *f*.

5.5. Effect of PFPA content on non-planar HC film formation

Previous reports for a range of star polymers with varying T_g values (−123 to 100 °C) cast onto TEM grids (non-planar substrates) had suggested that the non-cracking behaviour of the HC films was restricted to polymers with T_g values of <48 °C [27]. Subsequently, we discovered that this is only true for certain polymer types and that the Young's modulus (E) of a polymer is a better indicator of its ability to form non-cracking HC films on non-planer substrates. An E of *ca.* 5 GPa was identified as a likely boundary, with polymers having lower E forming non-cracking HC films on non-planar surfaces. In this study, the E values of flat non-porous films cast from star polymers **4S$_{1-4}$**, **6S$_{1-4}$** and **21S$_{1-5}$** were measured *via* AFM and plotted against PFPA content and T_g (Fig. 6). The E values of the polymer films were found to decrease with increasing PFPA content (Fig. 6a), which indicates an efficient approach to controlling E by changing the PFPA content. Furthermore, the star polymers' T_g values ranged from 20.8 °C to 94.5 °C while having E values below 5.07 GPa (Fig. 6b). According to our hypothesis, all star polymers prepared in this study should be able to form non-cracking films on non-planar TEM grids [20].

To validate this hypothesis, star polymer solutions (5 mg/mL in chloroform) were cast onto TEM grids at 30 °C and 70% R.H. using the static casting method described previously (ESI, Scheme S2), and the resulting HC structures were analysed by SEM. All star polymers formed non-cracking HC films on TEM grids and displayed good conformity to the non-planar surfaces (Fig. 7).

These results strongly suggest that by increasing the amount of the PFPA component in the polymer, the elasticity can be effectively enhanced (Table 1). The resultant E determines the star polymer's ability to form non-cracking HC films on non-planar surfaces. Therefore with careful design, star polymers with different T_g and E can be targeted, by varying the PFPA content, that possess the ability to form HC films contouring to non-planar surfaces without cracking, making them good candidates for non-planar coating applications. These new insights are anticipated to aid the successful design of a range of polymer systems that can undergo the formation of non-cracking HC films on non-planar surfaces.

6. Conclusions

In this study, we investigated the formation of honeycomb films from a series of well-defined star polymers with 4, 6, and 21 arms and different fluorine contents. The results indicate the following important findings: (1) By increasing the fluorine content of the star polymers, the Young's modulus (E) of the honeycomb films can be effectively reduced, improving the ability of star polymers of forming non-cracking honeycomb films on non-planar surfaces. However, it was noted that very high fluorine content (>50 mol %) reduces the regularity of honeycomb structures. Therefore, to produce a suitable polymer to form both regular hexagonal structured and non-cracking honeycomb films, appropriate fluorine content needs to be determined. (2) With increasing fluorine content, the average pore diameter of the honeycomb structure decreased at different polymer solution concentrations and casting humidities. Decreased solution concentration and the increased humidity lead to an increase in average pore diameter, which is similar to that reported in the literature. (3) The glass transition temperatures (T_g) of the star polymers can be readily tuned by varying the fluorine content, which also has a strong influence on the wettability of the resulting honeycomb films. This work provides important insights into the effects of star polymer structure and PFPA content on their ability to form well structured honeycomb films *via* the Breath Figures technique, and allows the formulation of a range of high T_g polymers capable of forming homogeneous honeycomb films on non-planar surfaces.

Acknowledgements

Zhou Zhang wishes to thank CSIRO Office of Chief Executive (OCE) postgraduate scholarship and The University of Melbourne Eugen Singer Award. The author(s) would also like to acknowledge the Australian Research Council's Future Fellowship (FT110100411, G.G.Q.) and the Electron Microscopy Unit of the Bio21 Institute, The University of Melbourne, for their assistance with scanning electron microscopy performed throughout the course of this research.

Appendix A. Supplementary data

Supplementary data related to this article can be found at http://dx.doi.org/10.1016/j.polymer.2013.06.033.

References

[1] Escalé P, Rubatat L, Billon L, Save M. Eur Polym J 2012;48(6):1001–25.
[2] Hernández-Guerrero M, Stenzel MH. Polym Chem 2012;3(3):563–77.
[3] Sun H, Li W, Wu LX. Langmuir 2009;25:10466–72.
[4] De León AS, Rodríguez-Hernández J, Cortajarena AL. Biomaterials 2013;34(5):1453–60.
[5] Kawano T, Nakamichi Y, Fujinami S, Nakajima K, Yabu H, Shimomura M. Biomacromolecules 2013;14(4):1208–13.
[6] Akolekar D, Hind A, Bhargava S. J Colloid Interface Sci 1998;199(1):92–8.
[7] Lewandowski K, Murer P, Svec F, Fréchet JM. Anal Chem 1998;70(8):1629–38.
[8] Nishikawa T, Arai K, Hayashi J, Hara M, Shimomura M. Int J Nanosci 2002;1(5 and 6):415–8.
[9] Deutsch M, Vlasov YA, Norris DJ. Adv Mater 2000;12(16):1176–80.
[10] Hedrick JL, Miller RD, Hawker CJ, Carter KR, Volksen W, Yoon DY, et al. Adv Mater 1998;10(13):1049–53.
[11] Rayleigh L. Nature 1911;86(2169):416–7.

[12] Cheng C, Tian Y, Shi Y, Tang R, Xi F. Macromol Rapid Commun 2005;26(15):1266–72.
[13] Hayakawa T, Horiuchi S. Angew Chem Int Ed 2003;42(20):2285–9.
[14] De Boer B, Stalmach U, Nijland H, Hadziioannou G. Adv Mater 2000;12(21):1581–3.
[15] Widawski G, Rawiso M, Francois B. Nature 1994;369(6479):387–9.
[16] Song L, Bly RK, Wilson JN, Bakbak S, Park JO, Srinivasarao M, et al. Adv Mater 2004;16(2):115–8.
[17] Nishikawa T, Nishida J, Ookura R, Nishimura SI, Wada S, Karino T, et al. Mater Sci Eng C 1999;8:495–500.
[18] Saito Y, Kawano T, Shimomura M, Yabu H. Macromol Rapid Commun 2013;34(8):630–4.
[19] Cheng CX, Tian Y, Shi YQ, Tang RP, Xi F. Langmuir 2005;21(14):6576–81.
[20] Zhang Z, Hughes TC, Gurr PA, Blencowe A, Hao X, Qiao GG. Adv Mater 2012;24(31):4327–30.
[21] Zhang Z, Hao X, Gurr PA, Blencowe A, Hughes TC, Qiao GG. Aust J Chem 2012;65(8):1186–90.
[22] Sun H, Li H, Bu W, Xu M, Wu L. J Phys Chem B 2006;110(49):24847–54.
[23] Yu Y, Ma Y. Soft Matter 2011;7(3):884–6.
[24] Yabu H, Shimomura M. Chem Mater 2005;17(21):5231–4.
[25] Tian Y, Liu S, Ding H, Wang L, Liu B, Shi Y. Polymer 2007;48(8):2338–44.
[26] Connal LA, Vestberg R, Hawker CJ, Qiao GG. Adv Funct Mater 2008;18(22):3706–14.
[27] Connal LA, Vestberg R, Gurr PA, Hawker CJ, Qiao GG. Langmuir 2008;24(2):556–62.
[28] Connal LA, Qiao GG. Soft Matter 2007;3(7):837–9.
[29] Connal LA, Qiao GG. Adv Mater 2006;18(22):3024–8.
[30] Connal LA, Gurr PA, Qiao GG, Solomon DH. J Mater Chem 2005;15(12):1286–92.
[31] Connal LA. Aust J Chem 2007;60(10):794.
[32] Li L, Li J, Zhong Y, Chen C, Ben Y, Gong J, et al. J Mater Chem 2010;20(26):5446–53.
[33] Li L, Zhong Y, Gong J, Li J, Chen C, Zeng B, et al. Soft Matter 2011;7(2):546–52.
[34] Li L, Zhong Y, Gong J, Li J, Huang J, Ma Z. J Colloid Interface Sci 2011;354(2):758–64.
[35] Wood K. Macromol Symp 2002;187(1):469–80.
[36] Berglin M, Wynne KJ, Gatenholm P. J Colloid Interface Sci 2003;257(2):383–91.
[37] Li Z, Xing Y, Dai J. Appl Surf Sci 2008;254(7):2131–5.
[38] Aulin C, Shchukarev A, Lindqvist J, Malmström E, Wågberg L, Lindström T. J Colloid Interface Sci 2008;317(2):556–67.
[39] Shi A, Koka S, Ullett J. Prog Org Coat 2005;52(3):196–209.
[40] Tran ND, Dutta NK, Roy Choudhury N. Polym Degrad Stab 2006;91(5):1052–63.
[41] Torrisi A, Tuccitto N, Maccarrone G, Licciardello A. Appl Surf Sci 2008;255(4):1527–30.
[42] Wang H, Fang J, Cheng T, Ding J, Qu L, Dai L, et al. Chem Commun 2007;7:877–9.
[43] Evans MDM, Prakasam RK, Vaddavalli PK, Hughes TC, Knower W, Wilkie JS, et al. Biomaterials 2012;32(12):3158–65.
[44] Chan GY, Hughes TC, McLean KM, McFarland GA, Nguyen X, Wilkie JS, et al. Biomaterials 2006;27(8):1287–95.
[45] Yabu H, Takebayashi M, Tanaka M, Shimomura M. Langmuir 2005;21(8):3235–7.
[46] Hertz H. J Reine Angew Mathematik 1882;92:156–71.
[47] Jee AY, Lee M. Polym Test 2010;29(1):95–9.
[48] Rosenbluth MJ, Lam WA, Fletcher DA. Biophys J 2006;90(8):2994–3003.
[49] Li J, Xiao H. Tetrahedron Lett 2005;46(13):2227–9.
[50] Liu X, Tian Z, Chen C, Allcock HR. Macromolecules 2012;45(3):1417–26.
[51] Liu C, Zhang Y, Huang J. Macromolecules 2008;41(2):325–31.
[52] Li Z, Li P, Huang J. J Polym Sci Part A: Polym Chem 2006;44(15):4361–71.
[53] Jiang X, Chen Y, Xi F. Macromolecules 2010;43(17):7056–61.
[54] Blencowe A, Tan JF, Goh TK, Qiao GG. Polymer 2009;50(1):5–32.
[55] Heideman M, Johnson D, Burrus C. ASSP Magazine, IEEE 1984;1(4):14–21.
[56] Escalé P, Save M, Lapp A, Rubatat L, Billon L. Soft Matter 2010;6(14):3202–10.
[57] Li L, Chen C, Li J, Zhang A, Liu X, Xu B, et al. J Mater Chem 2009;19(18):2789–96.
[58] Dong W, Zhou Y, Yan D, Mai Y, He L, Jin C. Langmuir 2009;25(1):173–8.
[59] Jiang X, Gu J, Shen Y, Wang S, Tian X. J Appl Polym Sci 2011;119(6):3329–37.
[60] Peng J, Han Y, Yang Y, Li B. Polymer 2004;45(2):447–52.
[61] Xu Y, Zhu B, Xu Y. Polymer 2005;46(3):713–7.
[62] Tian Y, Liu S, Ding H, Wang L, Liu B, Shi Y. Macromol Chem Phys 2006;207(21):1998–2005.
[63] Maruyama N, Koito T, Nishida J, Sawadaishi T, Cieren X, Ijiro K, et al. Thin Solid Films 1998;327:854–6.